Contribution from the Departments of Chemistry, University of Notre Dame, Notre Dame, Indiana 46556, and University of Southern California, Los Angeles, California 90089-0744, and Department of Physics, The Pennsylvania State University, University Park, Pennsylvania 16802

Control of Spin State in Iron(III) Porphyrinates. The Admixed Intermediate-Spin Case. Crystal Structure, Mössbauer, and Susceptibility Study of $[Fe(OEP)(3,5\text{-}Cl_2py)_2]ClO_4$

W. Robert Scheidt,*[1] Sarah R. Osvath,[1] Young Ja Lee,[1] Christopher A. Reed,*[2] Ben Shaevitz,[3] and Govind P. Gupta*[3,4]

Received August 31, 1988

The structural, magnetic, and Mössbauer characterization of the complex bis(3,5-dichloropyridine)(octaethylporphinato)iron(III) perchlorate, $[Fe(OEP)(3,5\text{-}Cl_2py)_2]ClO_4$, is reported. In the solid state, this species is an example of an admixed intermediate-spin iron(III) complex. The magnetic susceptibility and Mössbauer data have been fit in terms of the theory suggested by Maltempo. The experimental magnetic susceptibility and Mössbauer data can both be fit by using the common parameters $g_\perp = 4.3$ and $\zeta = 150\ cm^{-1}$. The solid-state structure of the complex has been determined by a single-crystal X-ray diffraction study. Crystal data for $[Fe(OEP)(3,5\text{-}Cl_2py)_2]ClO_4$: $FeCl_5O_4N_6C_{46}H_{50}$, $a = 9.564$ (2) Å, $b = 21.190$ (3) Å, $c = 22.991$ (3) Å, $Z = 4$, orthorhombic, space group *Pbcm*. The $[Fe(OEP)(3,5\text{-}Cl_2py)_2]^+$ ion has a required mirror plane of symmetry perpendicular to the porphyrin plane, which passes through two opposite porphinato nitrogen atoms. The two pyridine planes are both perpendicular to the mirror plane and hence have a mutually parallel orientation. The average of the equatorial bond distances in the six-coordinate molecule is $Fe\text{–}N_p = 1.994$ (10) Å. Axial Fe–N(py) bond lengths are 2.328 and 2.366 (4) Å. In frozen solution, neither EPR nor Mössbauer measurements provide evidence for any electronic state other than admixed intermediate spin. The apparent importance of the rotational orientation of the axial pyridine ligands and ligand basicity in determining the spin state of the iron atom is discussed.

Spin-state phenomena associated with (porphinato)iron derivatives have been recognized as an important aspect of the biological control of hemoprotein function.[5] Accordingly, our groups have carried out a number of investigations to understand the control and modulation of spin states. Among other investigations, we have studied the thermal spin equilibrium ($S = {}^1/_2$, $S = {}^5/_2$) displayed by the bis(3-chloropyridine)(octaethylporphinato)iron(III) complex.[6] Hill, Buchler, and co-workers[6b] initially reported temperature-dependent magnetic susceptibility data for three different bis(pyridine)(octaethylporphinato)iron(III) complexes, where the axial ligand was pyridine, 3-chloropyridine, or 4-aminopyridine. The 3-chloropyridine derivative shows the largest temperature-dependent magnetic moment variation, while the strongly basic 4-aminopyridine species is effectively low spin. We initially prepared the complex $[Fe(OEP)(3,5\text{-}Cl_2py)_2]ClO_4$ to further explore these thermal spin equilibria. We had expected that the use of the very low basicity pyridine, 3,5-dichloropyridine, would lead to a significant decrease in the energy gap between the doublet ground state and the higher energy sextet state. We thus anticipated a larger high-spin fraction at room temperature for $[Fe(OEP)(3,5\text{-}Cl_2py)_2]ClO_4$ relative to that of the previously characterized species. This notion was quickly dispelled by the observed room-temperature magnetic moment of 4.4 μ_B, which is lower than had been observed for previously characterized species: 4.7 μ_B for $[Fe(OEP)(3\text{-}Cl\text{-}py)_2]ClO_4$.[6] An explanation for this unexpectedly low magnetic moment came from the powder EPR spectrum. The solid-state EPR spectrum is axial with $g_\perp \approx 4.2$, indicating an electronic state inconsistent with a thermal spin-equilibrium system, i.e. an admixed intermediate-spin state[7] for iron(III).

We have previously noted that an axial ligand orientation in which the angle ϕ[8,9] of a pyridine plane relative to the nearest $N_p\text{–}M\text{–}N_p$ coordinate plane has a value near zero degrees is incompatible with a low-spin state and must lead to either a high-spin or an admixed intermediate-spin state. Indeed, previous results led us to suggest that the orientation of the axial ligand planes with respect to the $Fe\text{–}N_p$ bonds could be the controlling factor in the spin state exhibited in bisligated iron(III) porphyrinate derivatives.[10] $[Fe(OEP)(3,5\text{-}Cl_2py)_2]ClO_4$ appeared to provide us with an additional example to test these ideas. Accordingly, we have determined the molecular structure of $[Fe(OEP)(3,5\text{-}Cl_2py)_2]ClO_4$ in order to define the axial ligand plane orientations. We have also measured the temperature-dependent magnetic susceptibility and the Mössbauer spectrum under a variety of temperatures and applied magnetic fields. All solid-state measurements are consistent with the assignment of an admixed intermediate-spin state to $[Fe(OEP)(3,5\text{-}Cl_2py)_2]ClO_4$.

In addition, we have measured the EPR and Mössbauer spectra of $[Fe(OEP)(3,5\text{-}Cl_2py)_2]ClO_4$ in frozen solution. Both sets of solution measurements are consistent with an admixed intermediate-spin species as the predominant species present. Neither shows the presence of any low-spin species.

Experimental Section

$[Fe(OEP)(OClO_3)]$ (0.30 g, 0.435 mmol) and 3,5-dichloropyridine (0.20 g, 1.35 mmol) in 40 mL of benzene (dried over sodium benzophenone ketyl) was refluxed overnight and cooled to room temperature. After removal of most of the benzene under vacuum, the product was collected on a medium-porosity glass frit and washed with portions of dry heptane to remove excess ligand. Single crystals of the complex were prepared by slow vapor diffusion of heptane into a benzene solution. Well-formed crystals of this sample (**1**) were used for initial Mössbauer measurements and the X-ray diffraction study. Two additional samples were prepared analogously (**2** and **3**), with sample **3** having been recrystallized from chloroform/hexane. Several additional samples (**4**–**10**) were prepared (at about ${}^1/_{10}$th of the scale above) by dissolving the two reagents in the minimum amount of solvent (chloroform, chlorobenzene, or fluorobenzene) and then diffusing in dry hexane in a closed container. All products were crystalline material of varying crystallite size.

Magnetic susceptibility measurements were performed on finely ground samples tightly packed into aluminum buckets. Data were taken from 1.9 to 300 K in a field of 1.0 T on an SHE Model 905 SQUID susceptometer and are displayed graphically in the text. Actual data are available as Table 1S of the supplementary material. EPR spectra were measured in frozen methylene chloride solution at 11 K on an IBM

(1) University of Notre Dame.
(2) University of Southern California.
(3) The Pennsylvania State University.
(4) On leave from the Physics Department, Lucknow University, Lucknow, India.
(5) Scheidt, W. R.; Reed, C. A. *Chem. Rev.* **1981**, *81*, 543.
(6) (a) Scheidt, W. R.; Geiger, D. K.; Haller, K. J. *J. Am. Chem. Soc.* **1982**, *104*, 495. (b) Hill, H. A. O.; Skyte, P. D.; Buchler, J. W.; Lueken, H.; Tonn, M.; Gregson, A. K.; Pellizer, G. *J. Chem. Soc., Chem. Commun.* **1979**, 151. (c) Gregson, A. K. *Inorg. Chem.* **1981**, *20*, 81.
(7) Maltempo, M. M.; Moss, T. H. *Q. Rev. Biophys.* **1976**, *9*, 181.
(8) The use of the dihedral angle ϕ, defined by the ligand plane and the coordinate plane composed of a porphinato nitrogen atom (N_p), the metal atom (M), and the axial donor atoms, was originally suggested[9] by Hoard and co-workers.
(9) Collins, D. M.; Countryman, R.; Hoard, J. L. *J. Am. Chem. Soc.* **1972**, *94*, 2066.
(10) Scheidt, W. R.; Geiger, D. K.; Hayes, R. G.; Lang, G. *J. Am. Chem. Soc.* **1983**, *105*, 2625.

0020-1669/89/1328-1591$01.50/0

Table I. Fractional Coordinates for $[Fe(OEP)(3,5\text{-}Cl_2py)_2]ClO_4$[a]

atom	x	y	z
Fe	0.79630 (7)	0.039892 (27)	0.7500
Cl(1)	0.29636 (12)	0.13797 (5)	0.63333 (5)
Cl(2)	1.31590 (11)	−0.03906 (5)	0.63302 (4)
Cl(3)	0.18681 (24)	0.2500	0.5000
N(1)	0.8708 (4)	0.12777 (15)	0.7500
N(2)	0.79660 (27)	0.03988 (11)	0.66369 (11)
N(3)	0.7234 (4)	−0.04877 (15)	0.7500
N(4)	0.5705 (4)	0.08087 (16)	0.7500
N(5)	1.0299 (4)	0.00311 (16)	0.7500
C(a1)	0.9058 (3)	0.16382 (14)	0.70216 (14)
C(a2)	0.8317 (4)	0.08924 (16)	0.62699 (14)
C(a3)	0.7575 (4)	−0.00886 (16)	0.62692 (15)
C(a4)	0.6968 (3)	−0.08625 (14)	0.70204 (15)
C(b1)	0.9666 (3)	0.22323 (14)	0.72039 (13)
C(b2)	0.8100 (5)	0.07182 (19)	0.56765 (17)
C(b3)	0.7666 (5)	0.01069 (19)	0.56741 (16)
C(b4)	0.6484 (3)	−0.14783 (14)	0.72071 (15)
C(m1)	0.8865 (4)	0.14625 (15)	0.64532 (15)
C(m2)	0.7135 (4)	−0.06774 (15)	0.64510 (15)
C(1)	0.5054 (4)	0.09426 (15)	0.70011 (15)
C(2)	0.3727 (4)	0.12091 (15)	0.69906 (17)
C(3)	0.3049 (5)	0.13414 (22)	0.7500
C(4)	1.0978 (3)	−0.00693 (15)	0.70010 (14)
C(5)	1.2338 (3)	−0.02781 (14)	0.69891 (14)
C(6)	1.3059 (5)	−0.03860 (21)	0.7500
C(11)	1.0216 (4)	0.27260 (16)	0.68012 (16)
C(12)	0.9139 (6)	0.31702 (22)	0.65682 (25)
C(21)	0.8239 (8)	0.11632 (27)	0.51661 (19)
C(22)	0.7022 (12)	0.1586 (3)	0.5090 (3)
C(31)	0.7424 (7)	−0.03276 (26)	0.51554 (20)
C(32)	0.8674 (17)	−0.0617 (5)	0.4955 (5)
C(32)′	0.6023 (15)	−0.0373 (7)	0.5041 (6)
C(41)	0.6132 (4)	−0.20117 (16)	0.68056 (19)
C(42)	0.4626 (6)	−0.20552 (26)	0.6637 (3)
O(1)	0.1160 (8)	0.27956 (28)	0.45904 (20)
O(2)	0.2653 (9)	0.2054 (3)	0.4731 (4)

[a] The estimated standard deviations of the least significant digits are given in parentheses.

ER/200D spectrometer equipped with an Oxford Industries cryostat. Measurements were made on solutions with both stoichiometric and excess axial ligand present.

Mössbauer spectra were gathered on polycrystalline samples or solutions in horizontal transmission geometry in the temperature range 1.54–300 K and at fields varying from 0 to 6 T. All shifts are reported relative to metallic iron. Complete details of the experimental setup have been published.[11] Solutions for Mössbauer measurements were prepared by dissolving 50 mg of $[Fe(OEP)(OClO_3)]$ in 6 mL of fluorobenzene and then adding sufficient 3,5-dichloropyridine to have a stoichiometric quantity or a 2- or 10-fold excess of axial ligand. Such solutions were quickly frozen by immersion in liquid nitrogen and used immediately. Solution Mössbauer measurements were made at 77 and 4.2 K.

Preliminary examination of single crystals of $[Fe(OEP)(3,5\text{-}Cl_2py)_2]ClO_4$ were carried out on an Enraf-Nonius CAD4 automated diffractometer and led to the assignment of a four-molecule orthorhombic unit cell. An isosceles-triangular-shaped crystal with a thickness of 0.11 mm, a base of 0.33 mm, and sides of 0.55 mm was used for all measurements. The systematic absences are consistent with the centrosymmetric space group *Pbcm* (No. 59) or the noncentrosymmetric alternative $Pca2_1$. Least-squares refinement of the setting angles of 25 reflections with $23.0 < 2\theta < 29.8°$ led to the cell constants $a = 9.564$ (2) Å, $b = 21.190$ (3) Å, and $c = 22.991$ (3) Å. For a cell content of four $FeCl_5O_4N_6C_{46}H_{50}$, the calculated density is 1.403 g/cm³ and the measured density was 1.40 g/cm³.

Intensity data were measured on the CAD4 diffractometer using graphite-monochromated Mo Kα radiation and θ–2θ scanning at the ambient laboratory temperature of 293 ± 1 K. Three standard reflections were monitored every hour during data collection, with no significant deviations noted. Intensity data were reduced by application of standard Lorentz and polarization corrections but were not corrected for absorption ($\mu = 0.66$ mm⁻¹). A total of 3093 reflections having ($\sin\theta/\lambda < 0.65$ Å⁻¹ and $F > 3\sigma(F)$ were taken as observed.

The structure was solved in the centrosymmetric space group *Pbcm* by the direct-methods programs MULTAN78 and DIRDIF.[12] The resulting

(11) Lang, G. *Q. Rev. Biophys.* **1970**, *3*, 1.

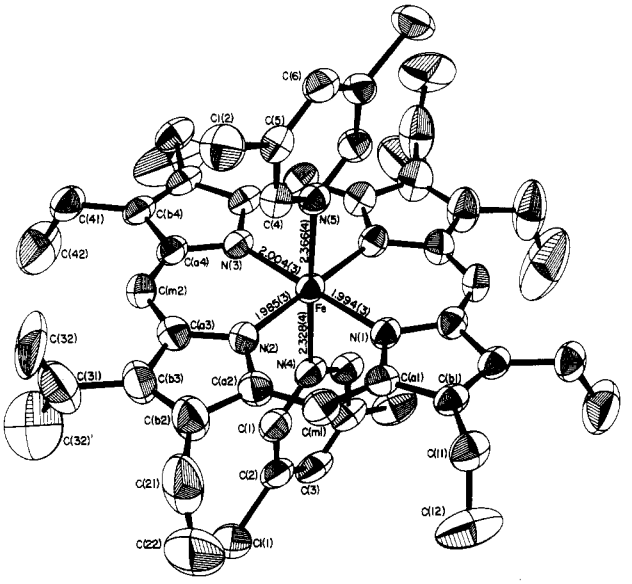

Figure 1. ORTEP diagram of $[Fe(OEP)(3,5\text{-}Cl_2py)_2]^+$ as it exists in the solid. The atom-labeling scheme for the crystallographically unique atoms and the bond distances in the coordination group are also illustrated.

Table II. Bond Distances (Å) in $[Fe(OEP)(3,5\text{-}Cl_2py)_2]ClO_4$[a]

Fe–N(1)	1.994 (3)	C(b1e–C(11)	1.493 (4)
Fe–N(2)	1.985 (3)	C(b2)–C(b3)	1.361 (5)
Fe–N(3)	2.004 (3)	C(b2)–C(21)	1.511 (6)
Fe–N(4)	2.328 (4)	C(b3)–C(31)	1.524 (6)
Fe–N(5)	2.366 (4)	C(b4)–C(b4)[m]	1.347 (7)
N(1)–C(a1)	1.381 (4)	C(b4)–C(41)	1.498 (5)
N(2)–C(a2)	1.385 (4)	C(1)–C(2)	1.390 (5)
N(2)–C(a3)	1.386 (4)	C(2)–C(3)	1.368 (4)
N(3)–C(a4)	1.383 (4)	C(2)–Cl(1)	1.717 (4)
N(4)–C(1)	1.336 (4)	C(4)–C(5)	1.375 (5)
N(5)–C(4)	1.335 (4)	C(5)–C(6)	1.381 (4)
C(a1)–C(b1)	1.448 (4)	C(5)–Cl(2)	1.723 (3)
C(a1)–C(m1)	1.371 (4)	C(11)–C(12)	1.495 (6)
C(a2)–C(b2)	1.428 (5)	C(21)–C(22)	1.480 (11)
C(a2)–C(m1)	1.383 (5)	C(31)–C(32)	1.421 (14)
C(a3)–C(b3)	1.432 (5)	C(31)–C(32)′	1.368 (14)
C(a3)–C(m2)	1.382 (5)	C(41)–C(42)	1.494 (6)
C(a4)–C(b4)	1.450 (4)	Cl(3)–O(1)	1.318 (4)
C(a4)–C(m2)	1.376 (5)	Cl(3)–O(2)	1.356 (6)
C(b1)–C(b1)[m]	1.362 (6)		

[a] The numbers in parentheses are the estimated standard deviations. C(32) and C(32)′ are disordered half-atoms. C(*2*) and C(*i*)[m] denote atoms related by the mirror plane.

E maps gave positions of most atoms; the crystallographically required mirror plane was found to be perpendicular to the porphyrin plane. Subsequent difference Fourier syntheses revealed that the terminal carbon atom of one ethyl group was disordered. Attempts to resolve the disorder by using the lower symmetry space group $Pca2_1$ were judged unsuccessful. In addition to higher discrepancy indices for the converged isotropic model, there was substantially poorer internal consistency for the parameters with the noncentrosymmetric space group. After least-squares refinement was carried to convergence, a difference Fourier suggested locations for all hydrogen atoms. All hydrogen atoms were included in subsequent cycles of least-squares refinement as fixed contributors (C–H = 0.95 Å and $B(H) = B(C) + 1.0$ Å²). Final cycles of

(12) Programs used in this study included Beurskens, Bosman, Doeburg, Gould, van den Hark, Prick, Noordik, Stempel and Smits' DIRDIF, Main, Hull, Lessinger, Germain, Declerq, and Woolfson's MULTAN78, local modifications of Jacobson's ALLS, Zalkin's FORDAP, Busing and Levy's ORFFE and ORELS, and Johnson's ORTEP2. Atomic form factors were from: Cromer, D. T.; Mann, J. B. *Acta Crystallogr., Sect. A* **1968**, *A24*, 321. Real and imaginary corrections for anomalous dispersion in the form factor of the iron and chlorine atoms were from: Cromer, D. T.; Liberman, D. J. *J. Chem. Phys.* **1970**, *53*, 1891. Scattering factors for hydrogen were from: Stewart, R. F.; Davidson, E. R.; Simpson, W. T. *Ibid.* **1965**, *42*, 3175. All calculations were performed on a VAX 11/730.

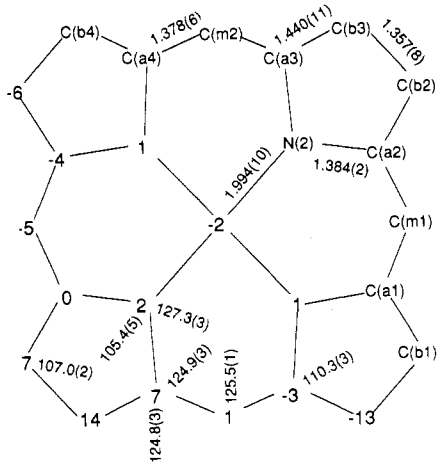

Figure 2. Formal diagram of the porphinato core in $[Fe(OEP)(3,5\text{-}Cl_2py)_2]^+$, illustrating the perpendicular displacements (in units of 0.01 Å) of each atom from the 24-atom porphinato core. Averaged values of the various chemical types of bond distances and bond angles in the porphinato core are also displayed.

full-matrix least-squares refinement used anisotropic temperature factors for all heavy atoms. At convergence, R_1 was 0.045, R_2 was 0.056, the error of fit was 1.71, and the final data/parameter ratio was 10.3. The highest peaks in the final difference map were around the perchlorate anion (0.3–0.4 e/Å^3). Final values of the atomic coordinates are listed in Table I. Complete details of the crystallographic work are available as Table 2S, while final values of the anisotropic temperature factors are listed in Table 3S of the supplementary material.

Results and Discussion

Molecular Structure. The molecular structure of the $[Fe(OEP)(3,5\text{-}Cl_2py)_2]^+$ ion is illustrated in Figure 1 along with the crystallographically unique bond distances around the iron. Bond distances and angles are listed in Tables II and III, respectively. Average values for each type of bond distance and bond angle in the porphinato core are shown in Figure 2. The number given in parentheses following each averaged value is the root-mean-square deviation from the average. Figure 2 also illustrates the displacements, in units of 0.01 Å, of each unique atom from the mean plane of the 24-atom core. As is readily seen, $[Fe(OEP)(3,5\text{-}Cl_2py)_2]ClO_4$ exhibits a modestly ruffled porphinato core. The small displacement of the iron atom of 0.02 Å is toward the pyridine ring with the longer Fe–N(py) bond distance.

The average Fe–N_p bond length of 1.994 (10) Å and the axial Fe–N(py) bond lengths of 2.328 (4) and 2.366 (4) Å are very similar to those of the intermediate-spin state form of $[Fe(OEP)(3\text{-}Cl\text{-}py)_2]ClO_4$[10] and to the equatorial bond distances of the other two known six-coordinate intermediate-spin ferric porphyrinates: $[Fe(OEP)(THF)_2]^+$[13] and polymeric $[Fe(TPP)(C(CN)_3)]_n$.[14]

The ion has a required mirror plane of symmetry that includes iron and two porphinato nitrogen atoms, N(1) and N(3), as well as the nitrogen and one carbon of each of the two axial ligands. The orientation of this mirror plane is notable on two points. In metalloporphyrin derivatives, crystallographically imposed mirror planes usually lie in the porphinato plane rather than perpendicular to it. However, the fact that the mirror has this particular perpendicular orientation leads to axial ligand orientations in which the projection of both pyridine planes exactly eclipse iron–porphinato nitrogen bonds. The mirror symmetry also requires that the two pyridine planes will have relative orientations in which they are either perpendicular or parallel to each other. In this complex the two planes are parallel. This is usually observed[15] relative orientation for bisligated metalloporphyrins, even for those derivatives having no crystallographically imposed symmetry.

Table III. Bond Angles (deg) in $[Fe(OEP)(3,5\text{-}Cl_2py)_2]ClO_4$[a]

N(1)–FeN(2)	89.98 (7)	C(a1)C(b1)C(b1)^m	106.82 (17)
N(1)–FeN(3)	179.41 (14)	C(a1)C(b1)C(11)	124.82 (29)
N(1)FeN(4)	89.04 (13)	C(b1)^{m}C(b1)C(11)	128.33 (18)
N(1)FeN(5)	88.29 (13)	C(a2)C(b2)C(b3)	107.1 (3)
N(2)FeN(2)^m	179.84 (15)	C(a2)C(b2)C(21)	124.6 (4)
N(2)FeN(3)	90.02 (7)	C(7b3)C(b2)C(21)	128.1 (4)
N(2)FeN(4)	90.08 (8)	C(a3)C(b3)C(b2)	106.8 (3)
N(2)FeN(5)	89.92 (8)	C(a3)C(b3)C(31)	124.3 (4)
N(3)FeN(4)	91.55 (13)	C(b2)C(b3)C(31)	128.7 (4)
N(3)FeN(5)	91.12 (13)	C(a4)C(b4)C(b4)^m	107.22 (19)
N(4)FeN(5)	177.33 (12)	C(a4)C(b4)C(41)	124.7 (3)
FeN(1)C(a1)	127.13 (17)	C(b4)^{m}C(b4)C(41)	128.05 (20)
C(a1)N(1)C(al)^m	105.6 (3)	C(al)C(m1)C(a2)	125.4 (3)
FeN(2)C(a2)	127.54 (21)	C(a3)C(m2)C(a4)	125.5 (3)
FeN(2)C(a3)	127.57 (22)	N(4)C(1)C(2)	121.8 (3)
C(a2)N(2)C(a3)	104.87 (26)	C(1)C(2)C(3)	120.1 (4)
FeN(3)C(a4)	127.06 (18)	C(1)C(2)Cl(1)	119.3 (3)
C(a4)N(3)C(a4)^m	105.8 (3)	C(3)C(2)Cl(1)	120.6 (3)
FeN(4)C(1)	120.77 (20)	C(2)C(3)C(2)^m	117.8 (5)
C(1)N(4)C(1)^m	118.4 (4)	N(5)C(4)C(5)	121.9 (3)
FeN(5)C(4)	120.76 (19)	C(4)C(5)C(6)	120.6 (3)
C(4)N(5)C(4)^m	118.5 (4)	C(4)C(5)Cl(2)	119.56 (26)
N(1)C(al)C(b1)	110.35 (28)	C(6)C(5)Cl(2)	119.83 (26)
N(1)C(a1)C(m1)	125.19 (28)	C(5)C(6)C(5)^m	116.5 (4)
C(b1)C(a1)C(m1)	124.46 (28)	C(b1)C(11)C(12)	114.9 (3)
N(1)C(a2)C(b2)	110.58 (29)	C(b2)C(21)C(22)	113.6 (6)
N(2)C(a2)C(m1)	124.5 (3)	C(b3)C(31)C(32)	112.8 (6)
C(b2)C(a2)C(m1)	124.9 (3)	C(b3)C(31),C(32)′	110.0 (8)
N(2)C(a3)C(b3)	110.54 (29)	C(32)C(31)C(32)′	136.9 (9)
N(2)C(a3)C(m2)	124.8 (3)	C(b4)C(41)C(42)	115.0 (4)
C(b3)C(a3)C(m2)	124.7 (3)	O(1)Cl(3)O(1)^n	118.2 (7)
N(3)C(a4)C(b4)	109.87 (29)	O(1)Cl(3)O(2)	106.8 (5)
N(3)C(a4)C(m2)	125.01 (28)	O(1)Cl(3)O(2)^n	106.2 (4)
C(b4)C(a4)C(m2)	125.12 (29)	O(2)Cl(3)O(2)^n	112.8 (9)

[a] The numbers in parentheses are the estimated standard deviations. C(32) and C(32)′ are disordered half-atoms. C(i) and C(i)^m denote atoms related by the mirror plane. C(i) and C(i)^n represent atoms related by the 2-fold symmetry axis.

Synthetic Aspects. Although the synthesis of $[Fe(OEP)(3,5\text{-}Cl_2py)_2]ClO_4$ would appear to be straightforward, difficulties were encountered in preparing pure bulk samples in quantities adequate for Mössbauer and magnetic susceptibility measurements. As illustrated in Table 5S, fully half of the preparations of $[Fe(OEP)(3,5\text{-}Cl_2py)_2]ClO_4$ were contaminated with a substance having different Mössbauer parameters (δ = 0.38–0.40 and ΔE = 0.87–0.97 mm/s at 77 K). On the basis of the Mössbauer parameters of the contaminant signal in zero and especially applied fields (vide infra), the contaminant is most likely a high-spin antiferromagnetically coupled species with $S = 0$. One expects this species to be $[Fe(OEP)]_2O$, although the quadrupole splitting does not quite agree with that given by Sams[16] (ΔE = 0.61 at 298 K and 0.82 at 4.2 K) for a pure sample. The variation in the amount of the contaminant signal shown by various partial samples of one bulk preparation as a function of crystallite size (sample 2 of Table 5S) is consistent with surface contamination. The difference in Mössbauer parameters from published μ-oxo values may be the result of a surface location as opposed to a discrete crystalline phase. A possible explanation for the ready formation of a μ-oxo impurity is the weakly basic nature of the 3,5-dichloropyridine ligand. It should be noted that techniques employed for the preparation of crystalline $[Fe(OEP)(3,5\text{-}Cl_2py)_2]ClO_4$ have been found to be fully adequate for the preparation of related complexes.

Magnetic Susceptibilities. The susceptibility of $[Fe(OEP)(3,5\text{-}Cl_2py)_2]ClO_4$ was measured in a 1.0-T field over the extended temperature range of 1.9–300 K. The effective number of Bohr magnetons, N_{eff}, has been plotted vs temperature in Figure 3. A logarithmic temperature scale has been used, since N_{eff} decreases rapidly at low temperature where the effects of zero-field splitting

(13) Masuda, H.; Taga, T.; Osaki, K.; Sugimoto, H.; Yoshida, Z.-I.; Ogoshi, H. *Bull. Chem. Soc. Jpn.* **1982**, *55*, 3891.
(14) Summerville, D. A.; Cohen, I. A.; Hatano, K.; Scheidt, W. R. *Inorg. Chem.* **1978**, *17*, 2906.
(15) Scheidt, W. R.; Lee, Y. J. *Struct. Bonding (Berlin)* **1987**, *64*, 1.
(16) Sams, J. R.; Tsin, T. B. *Porphyrins* **1979**, *4*, 454.

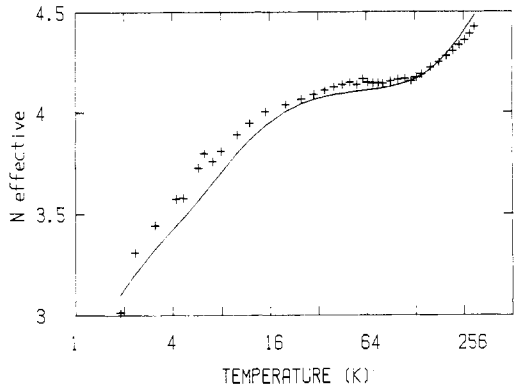

Figure 3. Experimental values (+) of N_{eff} as a function of temperature, where $N_{eff}^2 = 3kT\chi/\beta^2$ and χ is the susceptibility per heme unit. The data are fitted (solid curve) with the parameters $g_\perp = 4.3$ and $\zeta = 150$ cm^{-1} by using eq 1.

are most prominent. N_{eff} climbs from 3.02 at 1.9 K, levels to about 4.14 at 100 K, and then climbs to 4.43 at 300 K. Such temperature-dependent behavior is typical of a quantum-mechanically admixed intermediate-spin state. We have recently described the magnetic and Mössbauer parameters of a number of such admixed intermediate-spin states.[17-20]

The data displayed in Figure 3 were compared with those of the "Maltempo model"[7] by use of the Hamiltonian

$$\mathcal{H}_{el} = \Delta + \sum \zeta l_i \cdot s_i + 2\beta H \cdot S \qquad (1)$$

where the first term (Δ) is the energy gap between the $S = {}^3/_2$ and ${}^5/_2$ spin states, the second term represents the spin–orbit interaction with ζ as its one-electron coupling constant (summation over i is extended over all five 3d electrons of the ferric ion), and the last term is the Zeeman interaction of the electronic spin S ($=\sum s_i$) with the external field H.

The energy separation Δ can be related to the transverse gyromagnetic ratio $g_\perp$ of the lowest doublet, $S_z = \pm{}^1/_2$, by

$$\Delta = \pm\zeta\left[-\frac{24(g_\perp - 5)^2}{5(g_\perp - 6)(g_\perp - 4)}\right]^{1/2} \qquad (2)$$

where the lower sign applies for $g_\perp < 5$. Normally, $g_\perp$ is proportional to the magnetic splitting of the ground doublet and may be directly measured by EPR. Here, it may also be considered as a parameter indicating the percentage of the spin state $S = {}^3/_2$ in the admixed spin state. $g_\perp$ is linearly related to this percentage[7] with boundary values 0 and 100% corresponding to $g_\perp = 6$ and 4, respectively.

Theoretical values of N_{eff} obtained by using the parameters $g_\perp = 4.3$ and $\zeta = 150$ cm^{-1} are in good agreement with the experimental measurements displayed in Figure 3. The value of ζ is consistent with those obtained earlier for various admixed intermediate-spin complexes (see Table I of ref 19). The fitted $g_\perp$ value is in good agreement with the experimental EPR spectrum (crushed single crystals, 77 K), which has $g_\perp = 4.23$ and $g_\parallel = 2.00$.

Mössbauer Spectra. Mössbauer spectra of a pure sample of [Fe(OEP)(3,5-Cl_2py)$_2$]ClO_4 were recorded in zero field in the temperature range 1.54–300 K. Typical spectra are illustrated in Figure 4. The spectra were fitted by a least-squares minimization routine[21] with a Lorentzian line width w, a chemical shift δ(Fe), and a quadrupole splitting ΔE as free parameters. The value of δ varies from 0.30 to 0.41 mm/s as the temperature of the sample is lowered from 300 to 1.54 K. The variation is consistent with that expected from the usual second-order Doppler shift. The typical value of $\delta = 0.41$ mm/s at 4.2 K is that expected for iron in the ferric state. The value of $\Delta E = 3.12$ mm/s is independent of temperature within experimental accuracy. The large value of ΔE is suggestive of an admixed intermediate-spin state (see, for example, Table 1 of ref 19). The asymmetry of the quadrupole doublet is found to be temperature dependent. The line width ratio of the left-hand- and right-hand-side lines increases from 1.01 at 300 K to 1.86 at 1.54 K. Two typical spectra recorded at 300 and 4.2 K are shown in Figure 4. Normally the greater width is observed on the right-hand-side line (for ferric species with positive ΔE) and is assigned to the slowly relaxing $S_z = \pm{}^3/_2$ electronic levels. These levels produce a fluctuating field at the nucleus in the z direction and cause the $\pm{}^3/_2$ to $\pm{}^1/_2$ nuclear transitions to split more than the $\pm{}^1/_2$ to $\pm{}^1/_2$ transitions. In the present system it seems that the lowest lying Kramers doublet $S_z = \pm{}^1/_2$ relaxes with an intermediate rate and imposes a slowly fluctuating field at the nucleus in the xy plane. This causes the $\pm{}^1/_2$ to $\pm{}^1/_2$ nuclear transitions to split more than the $\pm{}^3/_2$ to $\pm{}^1/_2$ nuclear transitions and leads to the unusual asymmetry. The observation of an intermediate relaxation rate, even at 1.54 K and in zero applied field, strongly suggests that the ground state in this system is a Kramers doublet. Further, the broadening of the left-hand line confirms that the ground state is the $S_z = \pm{}^1/_2$ doublet, as only this can provide the fluctuating field in the xy plane, causing the broadening of the $\pm{}^1/_2$ to $\pm{}^1/_2$ nuclear transitions.

Mössbauer spectra of this complex recorded in high magnetic fields confirm the positive sign of the electric field gradient. The spectra were fitted in the "Maltempo model" by using a computer program described in detail elsewhere.[18] The computer simulations suggest that the spins fluctuate in the slow relaxation limit only when a magnetic field greater than 3 T is applied at a temperature less than 8 K. A typical spectrum at 4.2 K and 6 T is illustrated in Figure 4. The computer fitting of these spectra with the parameter values discussed above provides a hyperfine coupling constant of $P\kappa/g_N\beta_N = 12.83$ T/unit spin, consistent with its $g_\perp$ dependence as tabulated in Table 1 of ref 19.

From the detailed fits of the magnetic susceptibility and Mössbauer spectra of the several five-coordinate admixed intermediate-spin complexes[17-20] previously studied, all were found to have an antiferromagnetic interaction between paramagnetic centers. However, the low-temperature susceptibility measurements of [Fe(OEP)(3,5-Cl_2py)$_2$]ClO_4 indicate that no antiferromagnetic interaction of comparable magnitude is present. Indeed, the zero-field Mössbauer spectrum shows that even a small nuclear magnetic field (of the order of 1 mT) is sufficient to perturb the ground state and leads to an upper limit of 10^{-4} cm^{-1} for antiferromagnetic coupling. In large part, this difference in required antiferromagnetic coupling is explicable in terms of possible coupling paths. In all but one of the above mentioned cases, the probable coupling path involves a face-to-face porphyrin–porphyrin π–π interaction, a pathway clearly not available to a six-coordinated heme. However in one previous coupling case, that of the species [Fe(TPP)($FSbF_5$)]·C_6H_5F,[19] such a specific pathway was not apparent. Rather, a mean-field (nonpairwise) antiferromagnetic interaction was required to fit the data; a value of $-J = 1.4/n$ cm^{-1} was found to yield a good fit of the Mössbauer and low-temperature susceptibility data (n is the number of interacting spin systems). An explanation for the antiferromagnetic interaction in [Fe(TPP)($FSbF_5$)]·C_6H_5F and its absence in [Fe(OEP)(3,5-Cl_2py)$_2$]ClO_4 must lie in the differences in the solid-state intermolecular interactions, although both species have similar Fe···Fe distances and appear to have fairly well separated monomeric ions.

In order to determine the nature of the smaller quadrupole component present in many of the preparations (Table 5S), Mössbauer spectra of one of the impure samples of [Fe(OEP)(3,5-Cl_2py)$_2$]ClO_4 were recorded at 4.2 K in a 0- or 6-T magnetic field. The spectra were fitted with a modified program that could fit two components separately. A consistent fitting of both com-

(17) Gupta, G. P.; Lang, G.; Scheidt, W. R.; Geiger, D. K.; Reed, C. A. *J. Chem. Phys.* **1985**, *83*, 5945.
(18) Gupta, G. P.; Lang, G.; Scheidt, W. R.; Geiger, D. K.; Reed, C. A. *J. Chem. Phys.* **1986**, *85*, 5212.
(19) Gupta, G. P.; Lang, G.; Reed, C. A.; Shelly, K.; Scheidt, W. R. *J. Chem. Phys.* **1987**, *86*, 5288.
(20) Gupta, G. P.; Lang, G.; Lee, Y. J.; Scheidt, W. R.; Shelly, K.; Reed, C. A. *Inorg. Chem.* **1987**, *26*, 3022.
(21) Lang, G.; Dale, B. W. *Nucl. Instrum. Methods* **1974**, *116*, 567.

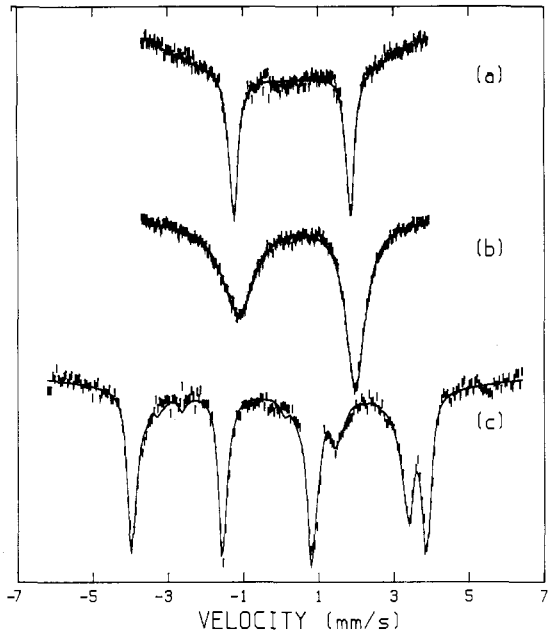

Figure 4. Mössbauer spectra: 300 K, 0 T (a); 4.2 K, 0 T (b); 4.2 K, 6 T (c). Spectrum a was fitted with δ = 0.31 mm/s (Fe), ΔE = 3.12 mm/s, and w = 0.29 and 0.27 mm/s. Spectrum b was fitted with δ = 0.41 mm/s (Fe), ΔE = 3.12 mm/s, and w = 1.09 and 0.62 mm/s. Spectrum c was fitted with δ = 0.41 mm/s (Fe), ΔE = 3.12 mm/s, w = 0.23 mm/s, $g_\perp$ = 4.3, ζ = 150 cm^{-1}, and $P\kappa/g_N\beta_N$ = 12.83 T/unit spin.

ponents of the spectra, displayed in Figure 5, confirms that one component (75%) is identical with that in the pure phase and the other (25%) has δ = 0.40 mm/s, ΔE = 0.96 mm/s, and S = 0. The values suggest that the second component is nonmagnetic; the most likely species would be high-spin antiferromagnetically coupled species such as μ-oxo.

Mössbauer spectra of frozen solutions of nominal [Fe(OEP)(3,5-Cl_2py)$_2$]$^+$ show two quadrupole-split doublets that are quite similar to those given in Table 5S. The proportion of the larger quadrupole-split doublet increases with increasing axial ligand concentration.[22] These spectra do not show any evidence for the formation a low-spin iron(III) complex. (All low-spin ferric species have isomer shifts less than 0.24 mm/s at 77 K.[16]) The absence of any low-spin species utilizing 3,5-dichloropyridine as an axial ligand was corroborated by EPR spectra of frozen solutions at 11 K. No low-spin component, either the normal low-spin type or the strong g_{max} signal,[23] was observed in the EPR spectrum. It thus appears that the bisligated species, [Fe(OEP)(3,5-Cl_2py)$_2$]$^+$, does not display a low-spin state under any experimentally accessible conditions that we are able to probe.

Axial Ligand Orientation and Basicity. We had previously noted[10] that low-spin pyridine-ligated iron(III) species, with required[5] short axial bonds, are commensurate only with ϕ values near 45°. On the other hand, high- or intermediate-spin-state species require long axial bond lengths that are, in principle, compatible with the entire range of ϕ values. Thus, the observed orientation of the pyridine ligands in [Fe(OEP)(3,5-Cl_2py)$_2$]$^+$ precludes a low-spin electronic state in the solid. However, the converse conclusion, that an admixed intermediate-spin state for iron requires the observed ligand orientation, is not definitively proven by these results. Nonetheless, all pyridine-ligated admixed intermediate-spin iron(III) porphyrinates (five independent structures)[10,24,25] have ϕ values near 0° and mutually parallel pyridine rings. Further, all are admixed intermediate-spin species with relatively small $S = {}^5/_2$ contributions. It is tempting to speculate that the degree of $S = {}^5/_2$ character in these admixed intermediate-spin species is related to the ϕ angle; increasing $S = {}^5/_2$ character would be found with larger ϕ angles. The one known high-spin species, that of the *excited state* of the thermal spin-equilibrium complex [Fe(OEP)(3-Cl-py)$_2$]ClO$_4$,[6] does have such a ligand orientation.

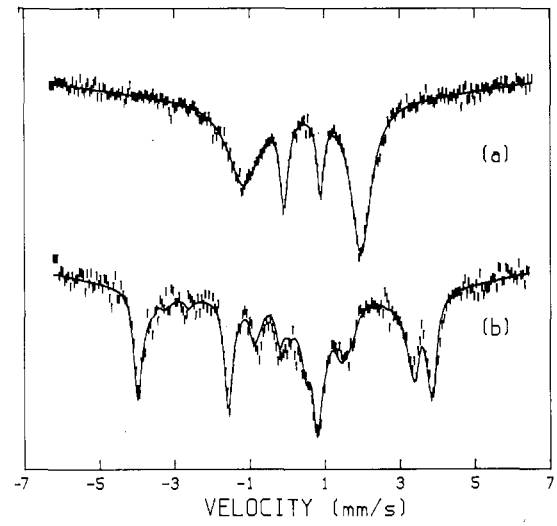

Figure 5. Mössbauer spectrum of an impure sample of [Fe(OEP)(3,5-Cl_2py)$_2$]ClO$_4$ at 4.2 K, 0 T (a) and 4.2 K, 6 T (b). Spectra were fitted with two components in the ratio of 3:1. The larger component has the same parameters as those given in Figure 4, and the smaller component has δ = 0.40 mm/s, ΔE = 0.96 mm/s, and S = 0.

Finally, we note that the failure to observe a low-spin state of [Fe(OEP)(3,5-Cl_2py)$_2$]$^+$ under any conditions suggests that for sufficiently weakly basic pyridine donors the electronic ground state for a bis(pyridine)-ligated iron(III) derivative is not an $S = {}^1/_2$ state. It thus appears that the use of relatively strongly basic pyridine derivatives as the axial ligands leads to a low-spin ground state, while lower basicity ligands yield admixed intermediate-spin ground states. The importance of pyridine ligand basicity to the observed spin state in bisligated iron(III) porphyrinates remains under active investigation.

Acknowledgment. We thank the National Institutes of Health for support of this work under Grants HL-16860 at Penn State, GM-38401 at Notre Dame, and GM-23851 at USC. We also thank Prof. George Lang for stimulating discussions and Martin Safo for preparing solutions for Mössbauer spectra.

Registry No. [Fe(OEP)(3,5-Cl_2py)$_2$]ClO$_4$, 119679-66-2; [Fe(OEP)(OClO$_3$)], 50540-30-2.

Supplementary Material Available: Table 1S, listing detailed magnetic susceptibility measurements for [Fe(OEP)(3,5-Cl_2py)$_2$]ClO$_4$, Table 2S, listing complete crystallographic details, Table 3S, listing anisotropic temperature factors, Table 4S, listing fixed hydrogen atom coordinates, and Table 5S, listing Mössbauer parameters for 10 different preparations of [Fe(OEP)(3,5-Cl_2py)$_2$]ClO$_4$ (5 pages); a table of observed and calculated (×10) structure factors (11 pages). Ordering information is given on any current masthead page.

(22) The observed value for the quadrupole doublet in frozen fluorobenzene solution (77 K) is 2.97 mm/s. The quadrupole doublet for pure [Fe(OEP)(OClO$_3$)] dissolved in fluorobenzene is 3.35 mm/s (77 K). This clearly suggests that the solution Mössbauer spectrum represents quadrupole splittings for [Fe(OEP)(3,5-Cl_2py)$_2$]$^+$ although another compound such as the mixed axial ligand species [Fe(OEP)(3,5-Cl_2py)(OClO$_3$)] is a (unlikely) possibility.

(23) Magita, C. T.; Iawizumi, M. *J. Am. Chem. Soc.* **1981**, *103*, 4378–4381. Walker, F. A.; Reis, D.; Balke, V. L. *J. Am. Chem. Soc.* **1984**, *106*, 6888–6898. Walker, F. A.; Huynh, B. H.; Scheidt, W. R.; Osvath, S. R. *J. Am. Chem. Soc.* **1986**, *108*, 5288–5297.

(24) Scheidt, W. R.; Geiger, D. K.; Lee, Y. J.; Reed, C. A.; Lang, G. *Inorg. Chem.* **1987**, *26*, 1039–1045.

(25) Safo, M.; Scheidt, W. R. Work in progress.